Journal of the Physical Society of Japan
Vol. 78, No. 8, August, 2009, 084723

Antiferromagnetic Resonance in Sodium Clusters in Sodalite

Takehito NAKANO*, Takanari KASHIWAGI[1†], Atsufumi HANAZAWA, Kunihiro WATANABE, Masayuki HAGIWARA[1], and Yasuo NOZUE

Department of Physics, Graduate School of Science, Osaka University, Toyonaka, Osaka 560-0043
[1]*KYOKUGEN (Center for Quantum Science and Technology under Extreme Conditions), Osaka University, Toyonaka, Osaka 560-8531*

(Received May 7, 2009; accepted June 12, 2009; published August 10, 2009)

Sodium clusters arrayed in aluminosilicate sodalite are known to show antiferromagnetism below the Néel temperature T_N of 48 K. We have performed electron spin resonance (ESR) measurements on a powder specimen of this material at an X-band microwave frequency (9.7 GHz) with temperature varying between 4 and 300 K. The ESR spectra show asymmetric broadening below T_N, which can be regarded as a powder pattern of the antiferromagnetic resonance (AFMR) signal. From the analysis of the AFMR fields at low temperatures using the exchange-coupling constants evaluated from the magnetic susceptibility, the anisotropy field is estimated to be significantly small at about 1–2 Oe. These results indicate that this material is an ideal Heisenberg antiferromagnet resulting from the character of s-electrons in zeolite cages with a cubic arrangement.

KEYWORDS: alkali-metal cluster, zeolite, sodalite, antiferromagnetic resonance, magnetic anisotropy, Heisenberg antiferromagnet
DOI: 10.1143/JPSJ.78.084723

1. Introduction

S-electrons can be accommodated in regularly arrayed nanospaces by loading alkali atoms into zeolite crystals, where s-electrons are confined in zeolite cages and are shared by several alkali cations to form nanoclusters. Exchange interactions between s-electrons in arrayed clusters have brought about magnetic orderings.[1–5] They are fascinating magnetic materials because the magnetically ordered states are realized by s-electrons of alkali metals without any magnetic elements such as transition metals. In the present work, we prepared sodium nanoclusters arrayed in sodalite, which is a type of aluminosilicate zeolite with a bcc arrangement of cages, that are known to show an antiferromagnetic long-range order (LRO),[2] and we performed electron spin resonance (ESR) measurements at various temperatures. We have succeeded in detecting the antiferromagnetic resonance (AFMR) signal in Na clusters in sodalite below the Néel temperature. The magnetic anisotropy was found to be quite small.

The framework of sodalite is built of oxygen-sharing AlO_4 and SiO_4 tetrahedra and has the SOD-type structure, as schematically shown in Fig. 1. β-Cages with an inside diameter of about 7 Å form a bcc structure with a lattice constant of 8.9 Å, and the bcc unit cell contains two β-cages. The number density of the β-cages is 3.0×10^{21} cm^{-3}. The framework ($Al_3Si_3O_{12}$) is negatively charged, and four Na^+ cations and one monovalent M^- anion such as Cl^- or OH^- are accommodated in the β-cage, resulting in the chemical formula of $Na_4MAl_3Si_3O_{12}$ per β-cage. After removing NaM and exposing it to sodium vapor, one Na atom is adsorbed into the β-cage and a Na_4^{3+} cationic cluster is formed in the β-cage, where one 3s-electron from the guest Na atom is shared by four Na^+ ions.[6] The optical spectra show a strong absorption peak at 2–2.5 eV, which is assigned to the optical transition from the a_1 (s-like) ground state to the t_2 (p-like) state of the cluster.[7,8] Srdanov *et al.* succeeded in forming Na_4^{3+} clusters in almost all β-cages, namely, nearly 100% occupation of the cages by s-electrons, and found the antiferromagnetic LRO below 48 K.[2] The magnetic phase transitions were confirmed by ^{27}Al- and ^{29}Si-NMR measurements,[9,10] and also by muon spin rotation (μSR)[11] studies. In ESR studies, a decrease in the electron paramagnetic resonance (EPR) signal intensity at approximately the Néel temperature was reported.[2] Mizoguchi and coworkers observed a steep increase in ESR linewidth below 50 K.[12,13] They attributed this behavior to the antiferromagnetic transition, but the signal observed below the Néel temperature was attributed to a paramagnetic resonance from the isolated electrons in an incompletely loaded part of the sample.[12] They might have failed to detect the main AFMR signal below T_N because they used rather low frequencies of several tens of MHz and 1 GHz for their ESR measurements. It is usually difficult to observe the broad AFMR signal of a powder sample at such low frequencies. Therefore, no information about the AFMR signal on these materials has been given so far. Scheuermann and coworkers pointed out that the temperature dependence of the local

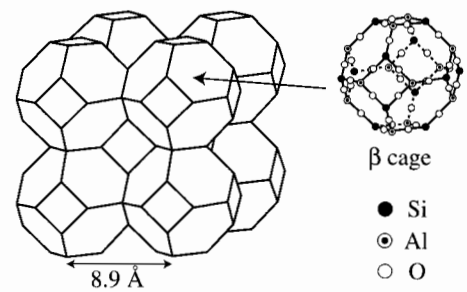

Fig. 1. Schematic illustration of the crystal structure of sodalite. The framework has the SOD-type structure. Cations distributed in the space of the framework are neglected here.

*E-mail: nakano@nano.phys.sci.osaka-u.ac.jp
†Present address: Institute of Materials Science, and Graduate School of Pure and Applied Sciences, University of Tsukuba, 1-1-1 Tennodai, Tsukuba, Ibaraki 305-8573.

internal field detected by μSR can be well explained by the three-dimensional Heisenberg model.[11] Generally, AFMR measurements have considerable advantage for detecting a small magnetic anisotropy. In the present paper, we report the results of AFMR measurements on a powder specimen of Na clusters in sodalite for the first time. The magnetic anisotropy was estimated to be quite small, indicating that this system is an ideal Heisenberg antiferromagnet.

2. Experimental Procedure

We used powder specimens of sodalite synthesized by Tosoh Corporation. Each crystal size was a few micrometers, and the chemical formula is given by $Na_4(OH)$-$Al_3Si_3O_{12}(H_2O)_2$ per β-cage. The NaOH unit was removed by Soxhlet extraction using pure water, and then $Na_3Al_3Si_3O_{12}(H_2O)_4$ was obtained. We abbreviate this NaOH-removed sodalite to Na-SOD hereafter. Na-SOD was fully dehydrated at 500 °C for about 24 h in vacuum. To produce Na clusters in sodalite, pure Na metal was adsorbed into dehydrated Na-SOD by heating at 160 °C for about two weeks in a sealed quartz tube. The average loading number of the guest Na atom, n, is one per β-cage. The value of n is equal to the average number of s-electrons per β-cage (or per cluster). We abbreviate the Na-SOD loaded with Na to Na/Na-SOD hereafter. Magnetization measurements were performed with a SQUID magnetometer (Quantum Design MPMS). ESR spectra were measured at an X-band microwave frequency (9.7 GHz) in the temperature range of 4–300 K by utilizing a Bruker EMX spectrometer equipped with an Oxford liquid helium flow cryostat. The ESR signal was taken by using a cylinder cavity in the TE_{011} mode and by sweeping the 100 kHz modulated external magnetic field with an amplitude of 1 Oe. Thus, we obtained the field derivative of ESR absorption.

3. Results and Discussion

Figure 2 shows the temperature dependence of the reciprocal magnetic susceptibility (χ) of Na/Na-SOD. In the high-temperature region, the susceptibility obeys the Curie–Weiss law shown by the straight line. The Curie constant is estimated to be 0.37 K emu/mol-cage. When all

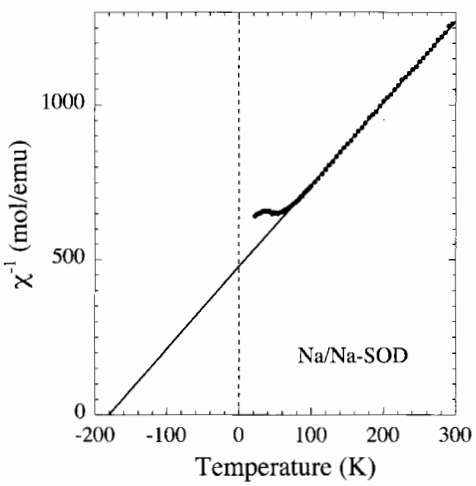

Fig. 2. Temperature dependence of the reciprocal magnetic susceptibility of Na/Na-SOD. The solid line shows the fitting result of the Curie–Weiss law.

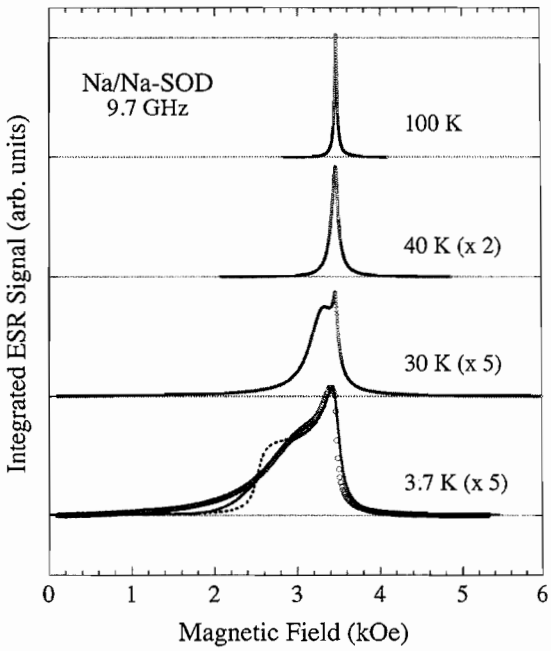

Fig. 3. (Color online) Temperature dependence of ESR spectra of Na/Na-SOD measured at 9.7 GHz. The results of simulation are also shown by the solid and the dashed curves for the lowest-temperature data.

of the β-cages are occupied by magnetic moments with spin quantum number $s = 1/2$ and g-value $g = 2$, the Curie constant is calculated to be 0.375 K emu/mol-cage. The observed value is very close to this value, indicating that each β-cage accommodates an unpaired electron with $s = 1/2$. The Weiss temperature estimated from the extrapolation of the straight line is -180 ± 5 K. At approximately 50 K, we observe the minimum of $1/\chi$, and hence the maximum of susceptibility. This temperature is close to the reported Néel temperature.[2,9–11] At temperatures lower than this minimum temperature, χ increases (or $1/\chi$ decreases) again. This is probably due to a paramagnetic contribution from uncompensated surface spins or some magnetic impurities, which give only a few percent of the total magnetic moments. The overall features of the magnetic susceptibility of our sample are consistent with those reported by other groups.[2,10,11]

Figure 3 shows the temperature dependence of the ESR spectra of Na/Na-SOD. The ESR spectra are field-integrated signals, namely, ESR absorption signals. For the lowest-temperature data, the results of the simulation are also shown by solid and dashed curves. The simulation method will be described later. At 100 K, which is in the paramagnetic region, a signal with a Lorentzian line shape, namely, an exchange-narrowed EPR signal,[13] is observed. The g-value is estimated to be 2.001. Upon cooling, the linewidth increases and the line shape changes significantly. As seen clearly in the lowest-temperature data, the spectral shape is asymmetric with a long tail on the low-field side. In Fig. 4, the full width at half maximum (FWHM) of the spectra is plotted on a logarithmic scale as a function of temperature. The linewidth rapidly increases below about 50 K, which coincides with the Néel temperature of 48 K. The linewidth at the liquid helium temperature is about 0.7 kOe. Note that the observed ESR spectra at low temperatures are much broader than that reported by Mizoguchi and coworkers.[12,13]

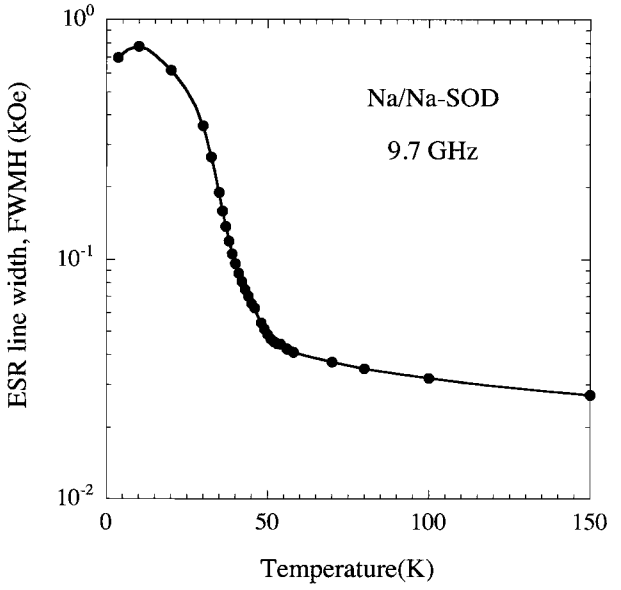

Fig. 4. Temperature dependence of the ESR linewidth (full width at half maximum) of Na/Na-SOD measured at 9.7 GHz. The width is plotted on a logarithmic scale.

The line broadening of the ESR spectra in Fig. 4 arises from the antiferromagnetic LRO, because the broadening starts at T_N. It is well known that the ESR linewidth at $T > T_N$ steeply increases with decreasing temperature in the vicinity of T_N owing to the development of the antiferromagnetic spin–spin correlation.[14,15] On the other hand, at $T < T_N$, the linewidth of the AFMR signal is known to decrease because of the reduction in the extent of magnon relaxation.[14] However, some of the AFMR modes deviate from the paramagnetic resonance mode depending on the field direction and the type of anisotropy. For powder samples, we detect the summation of the AFMR signals in all directions, because the sample orientation is distributed randomly, resulting in a broad and asymmetrical spectrum. This is certainly the case seen in Fig. 3. Actually, the asymmetrically broad spectra in Fig. 3 can be reproduced by simulating the powder pattern of the AFMR signals, as will be shown later.

The frequency dependence of the resonance fields depends on the type of magnetic anisotropy. Although we do not know the type of magnetic anisotropy in Na/Na-SOD, we extract the anisotropy field by assuming a simple case. As clearly shown in Fig. 3, the line broadening is significant on the low-field side. This is one of the characteristics in the case of easy-plane anisotropy, because there is no resonance mode at fields higher than that for the EPR line, as shown below. Hence, here we assume easy-plane anisotropy. According to the analytical calculation in the AFMR modes,[16] the resonance condition under an external magnetic field H is given by

$$\frac{(H\sin\theta)^2}{(\omega/\gamma)^2} + \frac{(H\cos\theta)^2}{(\omega/\gamma)^2 - 2H_E H_A} = 1, \tag{1}$$

in the case of easy-plane anisotropy, where ω is the angular frequency, γ is the gyromagnetic ratio of electronic spin ($\gamma\hbar = g\mu_B$), θ is the angle between the hard axis and the external field, namely, the polar angle, H_E is the exchange field, and H_A is the anisotropy field. From this relation, the respective resonance fields for the magnetic fields perpendicular ($\theta = 0$) and parallel ($\theta = \pi/2$) to the easy plane are given by

$$H_\perp = \sqrt{(\omega/\gamma)^2 - 2H_E H_A}, \tag{2}$$

$$H_\parallel = \omega/\gamma. \tag{3}$$

In a powder sample, one can expect a resonance field distribution in the range $H_\perp \le H \le H_\parallel$ because the crystals are randomly oriented. Hence, this gives a broad spectrum. From eqs. (2) and (3), the anisotropy field can be written as

$$H_A = \frac{H_\parallel^2 - H_\perp^2}{2H_E}. \tag{4}$$

The exchange field $H_E = 2z_1|J_1|s/g\mu_B$, where z_1 and J_1 (< 0, AF) indicate the number of nearest neighbors and the exchange-coupling constant between them, respectively, is evaluated from magnetic susceptibility. According to molecular field theory, the Néel temperature T_N and Weiss temperature Θ are given by

$$T_N = -2(z_1J_1 - z_2J_2)\frac{s(s+1)}{3k_B},$$
$$\Theta = 2(z_1J_1 + z_2J_2)\frac{s(s+1)}{3k_B}, \tag{5}$$

where J_2 and z_2 indicate the exchange-coupling constant between second-nearest neighbors and the number of second-nearest neighbors, respectively. The values of z_1 and z_2 are respectively eight and six in the bcc lattice. The spin quantum number s is 1/2, as mentioned above. When we substitute $T_N = 48$ K and $\Theta = -180$ K for the Néel and Weiss temperatures, respectively, the exchange-coupling constants are evaluated to be $J_1/k_B = -29$ K and $J_2/k_B = -22$ K. From these values, the exchange field is calculated to be $H_E = 1.7 \times 10^3$ kOe. When we choose the resonance fields $H_\parallel$ and $H_\perp$ as inflection points of the signal at the liquid helium temperature, $H_\parallel = 3.47$ kOe and $H_\perp = 2.77$ kOe are extracted from the data, and the anisotropy field is estimated to be $H_A = 1.3$ Oe using eq. (4). The obtained anisotropy is extremely small, indicating that this material is an isotropic Heisenberg antiferromagnet.

In the above, we discussed the magnetic anisotropy on the basis of the AFMR fields estimated from the inflection points of the absorption signal that correspond to the principal axes or planes. To strengthen the above discussion, we also carried out a simulation of the powder spectral pattern to reproduce the observed AFMR signal in the following manner. We also assume the easy-plane anisotropy here. The spectral pattern is given by the integration of the absorption lines over whole field directions with taking into account the resonance condition described by eq. (1). In a powder sample, there is a large number of particles oriented randomly. When the total number of particles is N_0, the number of particles oriented at a certain angle between θ and $\theta + d\theta$ is $(1/2)N_0 \sin\theta d\theta$, which can be easily derived from geometrical calculations. This number corresponds to the absorption intensity $W(H)$ at a certain magnetic field between H and $H + dH$, because only the corresponding particles satisfy the resonance condition. Therefore, $W(H)dH = (1/2)N_0 \sin\theta d\theta$, and then, the AFMR absorption intensity of a powder sample is given as

$$W(H) = \frac{1}{2} N_0 \sin\theta \frac{\mathrm{d}\theta}{\mathrm{d}H}. \tag{6}$$

The relation between θ and H is decided by the resonance condition of eq. (1), which can be rewritten as

$$\sin\theta \frac{\mathrm{d}\theta}{\mathrm{d}H} = \frac{A}{H}\sqrt{1 + A - B}, \tag{7}$$

where

$$\begin{aligned} A &= (\omega/\gamma)^2\{(\omega/\gamma)^2 - 2H_\mathrm{E}H_\mathrm{A}\}/2H_\mathrm{E}H_\mathrm{A}H^2, \\ B &= (\omega/\gamma)^2/2H_\mathrm{E}H_\mathrm{A}. \end{aligned} \tag{8}$$

Then, we can calculate the AFMR powder pattern in the case of easy-plane anisotropy using eqs. (6)–(8). In our calculation, the anisotropy of the g-value was ignored and the isotropic value of $g_\parallel = g_\perp = 2.00$ was used. For the exchange field, the value obtained from the susceptibility, $H_\mathrm{E} = 1.7 \times 10^3$ kOe, was used. The anisotropy field H_A was treated as a variable parameter. We also took into account the linewidth of each resonance mode mainly originating from relaxation processes. For this purpose, $W(H)$ was convoluted by a Lorenztian function $f(x)$ with a width of ΔH:

$$Y(H) = \int_{-\infty}^{\infty} f(H - H')W(H')\,\mathrm{d}H'. \tag{9}$$

This is the powder pattern signal. In accordance with the above method, we tried to reproduce the observed AFMR signal at low temperatures. The first simulation result is plotted as a dashed curve in Fig. 3 with the parameters $H_\mathrm{A} = 1.7$ Oe and $\Delta H = 150$ Oe. It can be seen that the spectral shape around the absorption peak top as well as the FWHM are well reproduced. There is, however, a discrepancy between the experimental and simulated spectra in the low-field-side tail. We could not reproduce the long tail on the low-field side at any value of H_A or ΔH. Then, we took into account the inhomogeneous distribution of the zero-field gap, which is given as $\sqrt{2H_\mathrm{E}H_\mathrm{A}}$ by substituting $H_\perp = 0$ in eq. (2). There may be some inhomogeneities in H_E and H_A in the sample due to the imperfection of the Na loading and for other reasons. Hence, the assumption of the zero-field-gap distribution is adequate. We assumed the distribution to be a Gaussian function. The result of the simulation is plotted as a solid curve in Fig. 3, where the parameters are $H_\mathrm{A} = 1.7$ Oe and $\Delta H = 150$ Oe, and the zero-field-gap distribution was assumed to have an 11% standard deviation. One can see that the overall spectral shape is well reproduced by the simulation. The obtained H_A is quite small and similar to the roughly estimated one discussed in the previous paragraph. The zero-field gap $\sqrt{2H_\mathrm{E}H_\mathrm{A}}$ is evaluated to be 2.3 kOe (6.5 GHz). In Fig. 5, the AFMR fields of Na/Na-SOD are plotted in the frequency vs magnetic field plane using the parameters obtained from the simulation. The X-band frequency (9.7 GHz) used in the present work is also indicated by the dash-dotted line in Fig. 5. Although we have found that the AFMR signal of Na/Na-SOD is well explained by easy-plane anisotropy, the single-frequency measurements might not be sufficient to unequivocally determine the type of anisotropy. Details of the anisotropy will be clarified by multi-frequency AFMR studies. Experiments to obtain such details are now in progress and will be reported elsewhere in the near future.

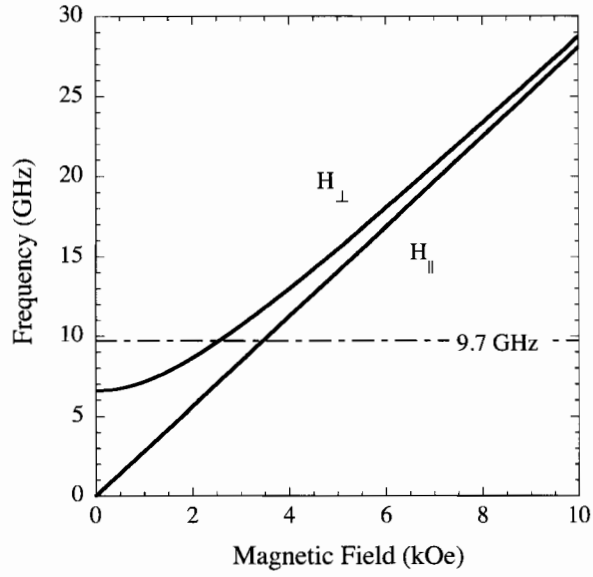

Fig. 5. Antiferromagnetic resonance fields of Na/Na-SOD in the frequency vs magnetic field plane. These are drawn using the parameters obtained from the powder spectral pattern simulation.

Generally, magnetic anisotropy originates from the symmetry of a crystal through spin–orbit interaction and/or a magnetic dipolar field. The β-cages of sodalite loaded with an alkali metal form a cubic structure, resulting in us expecting no such anisotropy. Moreover, guest electrons occupy an s-like (a_1) ground state with no angular momentum. The kinetic energy of the p-like (t_2) excited state is 2–3 eV higher than that in the ground state.[7,8] Hence, the spin–orbit interaction given by the second perturbation through the excited states is hardly expected. Actually, the observed g-values in the paramagnetic state are very close to $g = 2$. Therefore, we stress that the spin–orbit interaction cannot give an anisotropy in these systems. For the magnetic dipolar field, the magnetic anisotropy cannot be produced in these systems as long as the cubic symmetry is invariable down to the liquid helium temperature. Another possible cause of the small anisotropy is a hyperfine interaction between electronic and nuclear spins, which was reported in Mn^{2+} compounds with a cubic structure such as $KMnF_3$ and $RbMnF_3$.[17–19] Thus, we examine the possibility of the *hyperfine anisotropy* being the origin of the small anisotropy observed in sodalite loaded with an alkali metal. According to the EPR study of Na/Na-SOD with dilute Na loading, in which a small number of isolated Na_4^{3+} clusters are distributed, 13 hyperfine lines were observed at room temperature.[6] From these data, the hyperfine coupling constant was evaluated to be $A/g\mu_\mathrm{B} = 37.5$ Oe. By using this value and the ^{23}Na nuclear spin $I = 3/2$, the temperature dependence of the anisotropy field due to the hyperfine interaction is written as

$$H_\mathrm{A}^\mathrm{hf} = \frac{1}{g\mu_\mathrm{B}} \sum_j A_j^2 \frac{I_j(I_j+1)}{3k_\mathrm{B}T} s, \tag{10}$$

and is calculated to be $H_\mathrm{A}^\mathrm{hf} = 0.47/T$ (Oe) by taking into account the contributions of four ^{23}Na nuclei. According to our experimental data, the anisotropy field is estimated to be as large as 1–2 Oe even at 4 K, which is one order of magnitude larger than that of the calculated *hyperfine*

anisotropy. Hence, we cannot explain the observed anisotropy by the hyperfine interaction. The effect of the *hyperfine anisotropy* may appear at a sufficiently low temperature such as 100 mK. Consequently, we cannot unequivocally determine the origin of the small anisotropy at the present stage. One remaining possibility is that the crystal structure is slightly deformed from its cubic symmetry at low temperatures, which gives a small dipolar field anisotropy. Careful structural analysis at low temperatures may answer this question.

4. Conclusions

We performed ESR measurements on Na clusters in sodalite at an X-band frequency (9.7 GHz) at various temperatures. An asymmetric broad ESR signal was observed below the Néel temperature, which can be regarded as the powder pattern of the AFMR signals. From the analysis of the linewidth as well as AFMR powder pattern simulations and by considering the exchange-coupling constants, the magnetic anisotropy fields are found to be extremely small at 1–2 Oe. The origin of the anisotropy is not clear at the moment. This result indicates that this material is a quite ideal Heisenberg antiferromagnet.

Acknowledgments

We are grateful to Drs. K. Itabashi and M. Nakano (Tosoh Corporation) for providing high-quality sodalite crystals and to Mr. S. Tamiya (Osaka University) for conducting the chemical analysis. We also thank Emeritus Professor M. Date of Osaka University for his suggestion and encouragement. This work was partly supported by a Grant-in-Aid for Scientific Research on Priority Areas (Nos. 19051009 and 19051010), that for Scientific Research B (No. 20340089) and that for Young Scientists B (No. 20710077) from the Ministry of Education, Culture, Sports, Science and Technology, Japan (MEXT), and also by the 21st Century COE Program "Towards a New Basic Science: Depth and Synthesis" and the Global COE Program "Core Research and Engineering of Advanced Materials—Interdisciplinary Education Center for Materials Science", MEXT.

1) Y. Nozue, T. Kodaira, and T. Goto: Phys. Rev. Lett. **68** (1992) 3789.
2) V. I. Srdanov, G. D. Stucky, E. Lippmaa, and G. Engelhardt: Phys. Rev. Lett. **80** (1998) 2449.
3) T. Nakano, K. Goto, I. Watanabe, F. L. Pratt, Y. Ikemoto, and Y. Nozue: Physica B **374–375** (2006) 21.
4) T. C. Duan, T. Nakano, and Y. Nozue: J. Magn. Magn. Mater. **310** (2007) 1013; T. C. Duan, T. Nakano, and Y. Nozue: e-J. Surf. Sci. Nanotechnol. **5** (2007) 6.
5) T. Nakano and Y. Nozue: J. Comput. Methods Sci. Eng. **7** (2007) 443.
6) R. M. Barrer and J. F. Cole: J. Phys. Chem. Solids **29** (1968) 1755.
7) V. I. Srdanov, K. Haug, H. Metiu, and G. D. Stucky: J. Phys. Chem. **96** (1992) 9039.
8) N. P. Blake, V. I. Srdanov, G. D. Stucky, and H. Metiu: J. Chem. Phys. **104** (1996) 8721.
9) I. Heinmaa, S. Vija, and E. Lippmaa: Chem. Phys. Lett. **327** (2000) 131.
10) H. Tou, Y. Maniwa, K. Mizoguchi, L. Damjanovic, and V. I. Srdanov: J. Magn. Magn. Mater. **226–230** (2001) 1098.
11) R. Scheuermann, E. Roduner, G. Engelhardt, H.-H. Klauss, and D. Herlach: Phys. Rev. B **66** (2002) 144429.
12) K. Mizoguchi, K. Ichikawa, H. Sakamoto, Lj. Damjanovic, and V. I. Srdanov: Synth. Met. **103** (1999) 1877.
13) K. Mizoguchi, T. Takanashi, H. Sakamoto, Lj. Damjanovic, and V. I. Srdanov: Mol. Cryst. Liq. Cryst. **341** (2000) 467.
14) F. M. Johnson and A. H. Nethercot, Jr.: Phys. Rev. **114** (1959) 705.
15) H. Mori: Prog. Theor. Phys. **30** (1963) 578.
16) T. Nagamiya: Prog. Theor. Phys. **11** (1954) 309.
17) A. J. Heeger, A. M. Portis, D. T. Teaney, and G. Witt: Phys. Rev. Lett. **7** (1961) 307.
18) D. T. Teaney, M. J. Freiser, and R. W. H. Stevenson: Phys. Rev. Lett. **9** (1962) 212.
19) W. J. Ince: Phys. Rev. **177** (1969) 1005.